Food Research International 43 (2010) 1585–1593

Contents lists available at ScienceDirect

Food Research International

journal homepage: www.elsevier.com/locate/foodres

Influence of protein heat treatment on the continuous production of food foams

I. Nicorescu [a,*], C. Vial [b], C. Loisel [a], A. Riaublanc [c], G. Djelveh [b], G. Cuvelier [d], J. Legrand [e]

[a] GEPEA, ENITIAA, CNRS, UMR 6144, Rue de la Géraudière, BP 82225, 44322 Nantes Cedex 03, France
[b] CLERMONT UNIVERSITÉ, ENSCCF, LGCB, avenue des Landais, BP 206, 63174 Aubière Cedex, France
[c] BIA-INRA Nantes, Rue de la Géraudière, BP 71627, 44316 Nantes Cedex 03, France
[d] UMR SCALE, AgroParisTech, 1 rue des Olympiades, 91744 Massy Cedex 03, France
[e] GEPEA, University of Nantes, CNRS, UMR 6144, 37 bd de l'Université, BP 406, 44602 Saint Nazaire Cedex, France

ARTICLE INFO

Article history:
Received 8 January 2010
Accepted 12 March 2010

Keywords:
Dynamic heat treatment
Whey protein
Protein aggregation
Continuous aeration
Food foam
Foam stability

ABSTRACT

The influence of WPI heat treatment on the continuous production of food foams was investigated using a model food including xanthan. The temperature of heat treatment was increased up to 90 °C using a plate heat exchanger; a rotor–stator unit was used for aeration purpose. The aim was to determine the interplay between heat-induced protein denaturation and aggregation, and the process parameters of aeration operation: namely, rotation speed, residence time and operating pressure. Microstructure, texture and stability of 200% overrun foams were analysed. Experimental results demonstrated that foam microstructure, namely overrun and bubble size distribution, was governed by the process parameters of aeration and depended only slightly on thermal treatment. Conversely, foam stability was strongly improved by heat treatment. These trends agreed roughly with results obtained in a batch kitchen mixer, but batch methods remained unable to predict quantitatively the behaviours observed in continuous aeration operation.

1. Introduction

Many food products possessing an aerated structure are produced by beating air in a whipping device, i.e. using aeration. The main applications of aeration in the food industry include dairy and egg white-based products. Dairy products match mainly three classes: *acid* such as spreadable cheese and yogurt mousses, *frozen* such as ice cream and derivatives, and *neutral* such as whipped cream and sorbets. Egg white-based products include in particular meringue and nougat, but also cakes (sponge cake, angel food cake ...) and biscuits (lady finger biscuit ...). In aerated foods, the gas phase (usually air, but sometimes nitrogen), in forms of tiny bubbles, modifies not only the microstructure, but also the mouthfeel properties of the matrix in which it has been dispersed. Indeed, aeration may contribute to provide, for example, a specific textural character, such as brittleness in confectionary, lightness in whipped cream, or scoopability in vegetable and fish mousses (Bee, Clement, & Prins, 1987). However, bubbles also modify the visual aspect of foods that appear usually more bright and homogeneous, e.g. for duck liver mousses. In particular, for ice cream, aeration is coupled to freezing and, both simultaneously enhance the partial coalescence of fat droplets that governs creaminess (Marshall, Goff, & Hartel, 2003). Similarly, the quality of gas phase dispersion is a key element during the cooking of meringue or soufflés (Foegeding, Luck, & Davis, 2006). As a conclusion, gas acts as a functional ingredient in aerated food products.

Bubbles in food are usually stabilised by proteins, mainly egg white proteins, but also milk proteins, in particular whey proteins. This explains the growing interest for the use of whey protein isolate (WPI) as a food ingredient in aerated food (Zhu & Damodaran, 1994). Contrary to low-molecular-weight surfactants, proteins increase only moderately surface pressure, but are able to form cohesive and viscoelastic membranes at the air/water interface that prevent bubble coalescence (Saint-Jalmes, Peugeot, Ferraz, & Langevin, 2005). Proteins play therefore a key role, both on bubble breakup and stabilization, which is a strong function of their interfacial properties; however, these depend widely on the thermal treatments that have been applied to the recipe before aeration. For example, due to heat treatment, native β-lactoglobulin, the main protein in WPI, dissociates from a dimer to a monomer, exposing its thiol group and interior hydrophobic residues, and enabling thiol/disulfide exchange reactions; thus, denatured proteins may polymerise and form protein aggregates (Kazmierski & Correding, 2003). The resulting interfacial and foaming properties will therefore be a complex combination of the respective properties of aggregates, native and non-aggregated denatured proteins (Damodaran, 1997; Davis & Foegeding, 2004; Nicorescu et al., 2008b, Nicorescu et al., 2009a, Nicorescu et al., 2009b; Rullier, Novales, & Axelos, 2008; Schmitt, Bovay, Rouvet, Shojaei-Rami, & Kolodziejczyk, 2007; Unterhaslberger, Schmitt, Shojaei-Rami, & Sanchez, 2007). Zhu and Damodaran (1994) advocated that non-

* Corresponding author. Tel.: +33 251785469; fax: +33 251785467.
E-mail address: nicorescuirina@yahoo.com (I. Nicorescu).

0963-9969/$ - see front matter © 2010 Elsevier Ltd. All rights reserved.
doi:10.1016/j.foodres.2010.03.015

Nomenclature

DLS	dynamic light scattering
DSC	differential scanning calorimetry
Eff	effectiveness of aeration (%)
G	gas flow rate (atmospheric pressure, Nm^3/s)
G′, *G″*	viscoelastic shear moduli (Pa)
L	liquid flow rate (m^3/s)
RS	rotor–stator device
SEC	size-exclusion chromatography
t	time (s)
V	mixing head volume (m^3)
WPI	whey protein isolate

Greek letters

Φ	overrun (%)
ρ_F	foam density (kg/m^3)
ρ_L	solution density (kg/m^3)
τ	apparent residence time (s)

polymerised proteins contribute to foam formation as they diffuse more rapidly to the interfaces, while the aggregates act on foam stabilization because they can induce the subsequent formation of a viscoelastic network at the interface and even in thin films. According to Rullier, Novales, and Axelos (2008) and Nicorescu et al. (2008b), Nicorescu et al. (2009a), Nicorescu et al. (2009b), soluble protein aggregates with a size lower than 200 nm are mainly responsible for the enhancement of the foaming properties of whey proteins. Conversely, insoluble WPI aggregates were reported to impair these properties (Nicorescu et al., 2008b, Nicorescu et al., 2009a). This agrees roughly with the data of Zhu and Damodaran (1994) and Davis and Foegeding (2004): these authors claimed that only a limited heat treatment improved the foamability of protein solutions and foam stability, i.e. the foaming properties of WPI passed through a maximum as a function of the temperature of heat treatment and also as a function of the fraction of polymerised proteins.

The above-mentioned results are of utmost importance for the food industry that has always in mind the development of new innovative products. However, their practical applicability remains reduced. First, the foaming properties of proteins have usually been studied on the basis of "dry" foams in which the gas volume fraction is so high that bubbles are polyhedral and foam stability depends only on interfacial properties (i.e. thin-film properties), but this does not always match the situation encountered in the food industry: indeed, gas volume fraction is about 20–30% in liver mousses, 50% in ice cream and sorbets (Marshall et al., 2003), and 50–60% in whipped cream (Jakubczyk & Niranjan, 2006; van Aken, 2001); bubbles remain therefore spherical (although this can change during storage) and complementary mechanisms are necessary to ensure the shelf-life of the aerated structure: e.g. partial coalescence of fat droplets in whipped cream (Walstra, 2003), partial coalescence and freezing in frozen desserts (Marshall et al., 2003), cooking in meringue, viscosifiers and gelling agents in fruit fools and mousses ... The second key point is that batch heat treatment and aeration in kitchen mixers under atmospheric pressure are the rule in the literature, whereas dynamic heat treatment in plate heat exchangers and continuous aeration under pressure prevail in the food industry. However, only a few studies investigated either dynamic heat treatment (Nicorescu et al., 2008a, 2008b, Nicorescu et al., 2009a, Nicorescu et al., 2009b) or continuous aeration under steady state conditions (see, e.g. Djelveh & Gros, 1995; Hanselmann & Windhab, 1999; Thakur, Vial, & Djelveh, 2003; Müller-Fischer & Windhab, 2005; Indrawati, Wang, & Narsimhan, 2008b; Indrawati, Wang, Narsimhan, & Gonzalez, 2008a; Narchi, Vial, & Djelveh, 2007). In the food industry, aeration is typically carried out in axial rotor–stator mixers, using rotor and stator fitted with rows of pins (Hanselmann & Windhab, 1999; Labbafi et al., 2005; Müller-Fischer & Windhab, 2005), except for ice cream for which scraped surface heat exchangers prevail. From a practical point of view, rotor–stator devices are usually operated at high speed under pressure in the industry, although there is no proof that such a high shear and an energy input are required for aeration. Several attempts to establish a quantitative relationship between the operating conditions of continuous aeration (rotation speed, residence time ...), foam properties (overrun, bubble size distribution, stability ...) and mixer geometry have been reported in the literature (Djelveh & Gros, 1995; Narchi et al., 2007; Thakur, Vial, & Djelveh, 2005; Thakur et al., 2003), but the validity of their results is usually limited to the particular recipe studied in each of these works, and upstream heat treatment was not accounted for.

The objective of this work is therefore to investigate the influence of a dynamic heat treatment applied to WPI on the continuous production of a model aerated food, using a pilot-scale rotor–stator device that is representative of aeration equipment found in the food industry, in relation to the operating conditions applied during aeration: namely, rotation speed, residence time and operating pressure. The aim is to determine to which extent process parameters can or must be modified when heat-treated WPI are used in the recipe so as to ensure desired food properties, i.e. overrun, stability and texture. To approach a typical situation encountered in the food industry for WPI, overrun was limited to 200% (i.e. 66% gas volume fraction); xanthan was therefore added to WPI in the recipe to enhance the stability of the gas phase.

2. Materials and methods

2.1. Preparation of whey protein solutions

Commercial WPI Promilk® (83.35% w/w total protein, 2.9% minerals, <1% fat) was provided by *IDI Ingredients* (Arras, France) without further purification. The WPI powder contained 68% w/w β-lactoglobulin, 26.5% α-lactalbumin, 3.24% immunoglobulins and 0.69% bovine serum albumin. The powder was initially hydrated in deionised water for 2 h at 40 °C under mechanical stirring in order to prepare 3% w/v whey proteins solutions. pH was adjusted to 7.0 by a minute addition of a 1 M NaOH solution. The solution was then kept at 4 °C for 12 h to complete protein solubilisation. Then, the protein solutions were heat-treated at three different temperatures, 70 °C, 80 °C and 90 °C, respectively (as protein denaturation was negligible at 60 °C or below), in a 10-plate version of an *EXEL 2A* brazed plate heat exchanger based on a parallel flow configuration (*CIAT*, France). A single tube of 10 mm internal diameter was used as the holding section. The heat exchanger was fed using a peristaltic pump; the flow rate was 5 L/h and the length of the tube was adjusted to ensure 300 s holding time. The pH shift due to heat treatment was checked to remain always negligible. Similarly, clogging was never observed during heat treatment for these temperatures (i.e. up to 90 °C) and the amount of proteins lost in the plate heat exchanger was negligible. After heating, the samples were dynamically cooled at 15 °C using a 14 plate version of an *EXEL 2A* heat exchanger (*CIAT*, France). The required amount of sodium chloride was added to obtain the desired ionic strength

(50 mM). Unheated WPI solutions, denoted "native 3%-50 mM", could therefore be used as reference samples to analyse the influence of dynamic heat treatment. Measurements for the characterisation of proteins properties were immediately carried out. Then, 0.35% w/v xanthan gum was added under gentle agitation before storage at 4 °C. Viscosity measurements on the xanthan/protein solutions were carried out just before starting aeration experiments.

2.2. Micro-differential scanning calorimetry

Micro-differential scanning calorimetry (μDSC) was used to assess the degree of denaturation of whey proteins after heat treatment. μDSC thermograms of WPI solutions before and after the heat treatment were obtained using a Setaram III calorimeter (*Setaram Instrumentation*, France). Samples (700 mg) of the WPI solutions were hermetically sealed in a 1 mL hastelloy C276 pan. A closed pan filled with deionised water was used as the reference. The heating rate was fixed at 1.2 °C min^{-1} from 20 °C to 120 °C. All samples were analysed in duplicate. The degree of denaturation was calculated as a function of the surface area of the denaturation peak, i.e. it was estimated using the ratio between the specific enthalpy induced by the denaturation of the heated samples and the specific enthalpy value measured on the native sample.

2.3. Particle size analysis

2.3.1. Laser light diffraction

The size of protein aggregates larger than 50 nm can be measured by laser light diffraction, using a Mastersizer S apparatus (*Malvern Instruments*, UK) equipped with a 300 reverse Fourier lens and a He–Ne laser. The analysis requires the relative refractive index of the continuous (water) and the dispersed phase (whey protein aggregates): 1.33 and 1.52, respectively. Native and heat-treated WPI solutions were diluted with deionised water in the sample dispersion unit under stirring (1500 rpm). Volume-weighted particle size distributions of the protein aggregates were obtained using the Mie theory; measurements were carried out in triplicate.

2.3.2. Centrifugation step

To investigate the effect of the heat treatment on WPI solutions on the formation of soluble heat-induced aggregates, 20 mL of each sample were centrifuged at 10,000*g* for 30 min at 20 °C in a 2K15 centrifuge (*Sigma Laborzentrifugen GmbH*, Germany). This procedure ensured that the size of protein aggregates was lower than 1 μm in the supernatants, while aggregates larger than 1 μm remained in the solid. As a result, the soluble protein aggregates were separated from the insoluble fraction. This result was first validated by laser light diffraction (data not shown), which agrees with the data from Bench, Johnson, Hamilton, Gooch, and Wright (2004). After centrifugation, the soluble fractions were recovered for subsequent analysis and dry matter measurements were carried out after drying for 12 h at 102 °C in an oven, so as to quantify the amount of insoluble protein aggregates formed by heat treatment.

2.3.3. Dynamic light scattering (DLS)

The hydrodynamic diameters of soluble protein aggregates were measured in the supernatants by dynamic light scattering (DLS) using a Zetasizer Nano ZS Instrument (*Malvern Instruments*, UK). 2 mL of each sample of the WPI supernatants were thermostated to 20 °C before measurement in the Zetasizer. Experiments were carried out in triplicate.

2.4. Size-exclusion chromatography (SEC)

Twenty-five microlitres of the soluble protein fractions recovered from the supernatants of the centrifugation procedure were analysed by size exclusion chromatography (SEC) on a HPLC system (*Waters Corp*., MA, USA) equipped with a TSK 6000 column of 30 cm length (*Tosohaas*, PA, USA). Proteins were eluted with a pH 7 solution containing 0.05 M Tris and 0.1 M NaCl; the eluted proteins were detected using UV absorption at 280 nm; the amounts of non-aggregated proteins and aggregates were calculated on the basis of peak area measurements using the analysis software PeakFit (*Jandel Scientific Software*, USA).

2.5. Surface tension and viscosity

The surface tension σ of the protein solutions (2% w/v) was measured with a K12 tensiometer (*Krüss GmbH*, Germany) using the Wilhelmy's plate method at 10 °C for 3 h. The viscosity of the xanthan/protein mixtures was determined using an AR-1000 rheometer (*TA Instruments*, USA) using a Couette geometry (internal and external cylinder diameter: 2.76 cm and 3.00 cm, respectively) at 20 °C. Shear rate ranged between 50 s^{-1} and 1000 s^{-1}. Measurements for σ and viscosity were conducted in triplicate.

2.6. Continuous manufacturing of protein foams

A rotor–stator unit (RS) was employed for the continuous manufacturing of aerated food (Fig. 1). This unit consists of a 35 mm diameter stator and a 15 mm diameter rotor, both fitted with seven rows of squared pins (5 mm width). The length of the pins is 7.5 mm, which results in a pin-to-wall gap of 2.5 mm. The axial distance between rotor and stator rows of pins is also 2.5 mm and the volume available for the fluids is V = 180 mL. This geometry corresponds therefore to the scale-down of typical aeration equipment found in the food industry. Operating parameters consist of the flow rates of the liquid and the gas phases (L and G), the rotation speed of the rotor (N) and the operating pressure (P).

The xanthan/protein solutions based on native and heat-treated proteins, respectively, were used as the liquid phase. Gas and liquid phases were introduced separately from the bottom of the column. The liquid phase was fed using a peristaltic pump (*Cole-Parmer Instr. Corp*., USA); a mass flowmeter was used for the gas phase (*Emerson Brooks Inst*., USA). Rotation speed was varied from

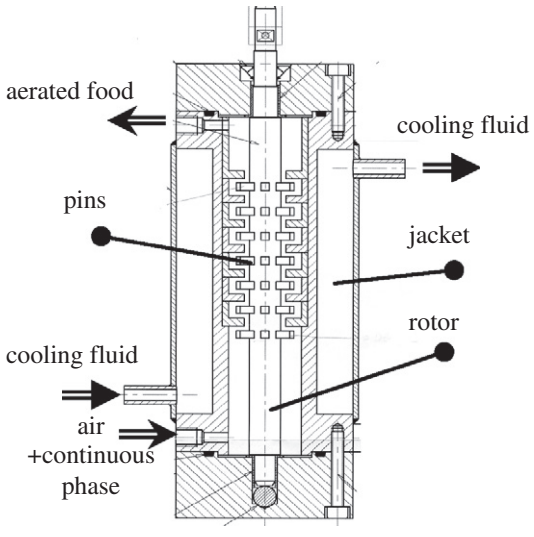

Fig. 1. Experimental set-up: axial rotor–stator unit.

400 to 1600 rpm using a speed-controlled IK LaborTechnik RE-16 engine (*Ika-Werke*, Germany). Gauge pressure in the RS unit could be controlled between 0 and 2 bars, using a backpressure valve placed on the outlet stream. For the liquid phase, the inlet temperature was kept constant at 4 °C; the RS unit was jacketed, so as to avoid heating by mechanical power dissipation (Balerin, Aymard, Ducept, Vaslin, & Cuvelier, 2007) and maintain the outlet temperature close to 4 °C; a WKL-600 thermocrysotat (*Lauda GmbH*, Germany) was used for circulating cooling fluid through the cooling jacket.

In this work, the gas-to-liquid flow rate ratio was kept constant at $G/L = 2$, expressing G values under atmospheric pressure. This defined the maximum foam overrun that could be achieved under steady state conditions, provided the gas phase was totally incorporated into the continuous one. Maximum overrun was therefore 200% (see Section 2.7 for details), which corresponds to a gas volume fraction of 66%. Consequently, only the apparent residence time τ (defined on G value at atmospheric pressure) was varied at constant G/L ratio:

$$\tau = \frac{V}{L+G} \quad (1)$$

With the assumption of total gas incorporation, foam residence time was varied between 40 s and 120 s, which correspond to L values between 30 and 90 mL/min (G values between 60 and 180 N mL/min, respectively).

2.7. Methods for foam characterisation

2.7.1. Overrun

The foaming ability of proteins was deduced first from overrun (Φ) measurements. The Φ values were derived from density measurements. Indeed, overrun can be expressed as follows:

$$\Phi = 100 \cdot \frac{\rho_L - \rho_F}{\rho_F} \quad [\%] \quad (2)$$

using the respective density of the solution (ρ_L) and the foam (ρ_F). The density of the foams was measured as the mass-to-volume ratio of the foam (sampled directly from the outlet stream of the RS unit) in a glass cup of known volume. Overrun was also used to check whether steady state conditions were achieved. Under continuous flow conditions, maximum overrun is equal to 100 G/L. The effectiveness of aeration *Eff* can therefore be defined as:

$$Eff = \Phi \cdot \frac{L}{G} \quad [\%] \quad (3)$$

2.7.2. Microstructure

The foaming ability of proteins was also deduced from the analysis of the bubble size distribution immediately after aeration. This was obtained on the basis of image analysis. Using a quartz cell placed on the outlet stream (Labbafi, Thakur, Vial, & Djelveh, 2007), photomicrographs were taken on-line using an inverted phase-contrast optical microscope (Axiovert-25, *Carl Zeiss Jena GmbH*, Germany) equipped with a CCD video camera (*Kappa Opto-Electronics GmbH*, Germany) and transferred to a computer. Then, the images were analysed using a dedicated analysis software, Image ProPlus 4.0 (*MediaCybernetics*, MD, USA). For each sample, at least 500 bubbles from several micrographs were detected and treated. This number was shown to be sufficient for statistical analysis, so that bubble size distribution and the average bubble size could be estimated automatically. The surface-average or Sauter mean diameter (d_{32}) was used to estimate the average bubble size (Labbafi et al., 2007).

2.7.3. Stability

Foam destabilization results from several phenomena, among which the most important are the gravitational drainage of the liquid phase and bubble coalescence. If bubble coalescence always contributes to foam collapse, foam drainage has a more ambiguous role because it can favour the formation of stable dry foams, whilst film thinning enhances bubble coalescence. In this work, foam collapse and liquid drainage were analysed independently. Drainage rate was determined by recording all the 10 s for a 3 h cycle the mass of liquid drained from a 127 mL glass cup filled of foam in a cylinder using a balance (Sartorius AG, Germany) connected to a computer. The kinetics of foam collapse was measured by following the evolution of foam height for 72 h in graduated 10 cm^3 tubes. These tubes were filled with foam using the outlet stream of the RS unit; they were stored at 4 °C and height measurements were carried out after 18, 48 and 72 h, respectively. All the foam drainage and collapse experiments were done in triplicate.

2.7.4. Texture

Rheological measurements were performed using a stress-controlled SR-5 rheometer (*Rheometric Scientific*, NJ, USA) equipped with a Peltier circulator for temperature control. The rheological characterisation of protein foams was carried out at 4 °C using a parallel plate geometry with 2 mm gap. Mechanical spectra in the linear viscoelastic domain were obtained from frequency sweep tests on foams in the 0.1–20 Hz range at 0.5% strain in order to analyse the texture of foams on the basis of the viscoelastic shear moduli, G' and G''. All the experiments were done in triplicate.

3. Results and discussion

3.1. Influence of heat treatment on proteins solutions

First, the degree of denaturation of proteins due to heat treatment in the plate heat exchanger has been quantified using μDSC. Experimental results (Table 1) shows that thermal treatment at 80 °C resulted in a nearly complete denaturation of the protein solutions, whereas samples heat-treated at 70 °C registered only 47% denaturation. This differs from the data of Nicorescu et al. (2009a) in which protein denaturation was negligible below 80 °C; these discrepancies may result first from a different protein content (2% w/v in Nicorescu et al. (2009a), vs. 3% w/v in this

Table 1
Properties of the WPI solutions before and after heat treatment.

Sample	Denaturation degree by DSC (%)	Protein fractions (% w/w)		Surface tension values at 3 h (mN/m)	Hydrodynamic diameter by DLS (nm)
		Soluble aggregates formed by heat treatment (SEC)	Insoluble aggregates (centrifugation)		
Native	–	–	1.1	39.6	122
70 °C	47	8	2.1	46.0	78
80 °C	97	14	8.8	47.0	107
90 °C	98	12	8.4	47.4	122

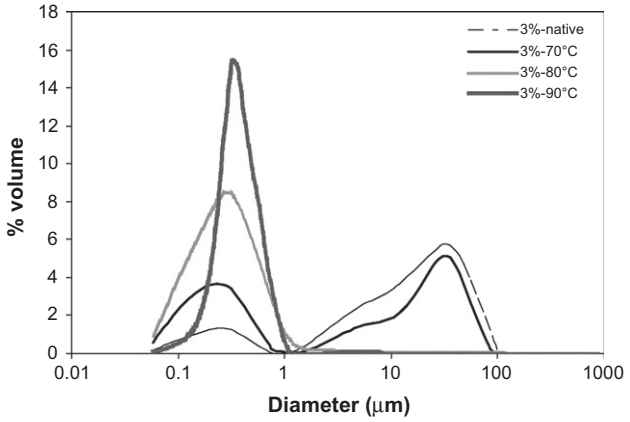

Fig. 2. Analysis of protein aggregation in native and heat-treated WPI solutions by laser light diffraction.

work), but also from the difference between the technologies used for heat treatment (a tubular heat exchanger in Nicorescu et al. (2009a) vs. a plate heat exchanger in this work).

Secondly, the insoluble protein fraction was quantified by centrifugation; data confirmed that the amount of insoluble aggregates increased suddenly when the temperature of the heat treatment was 80 °C and then did not vary significantly between 80 °C and 90 °C (Table 1), which is in good agreement with data on denaturation. Indeed, for 80 °C, protein denaturation was nearly complete, which favoured undoubtedly the interaction between denatured proteins via irreversible thiol-disulfide reactions, and thus the formation of larger protein aggregates. It is however worthy of note that some insoluble aggregates are already present with native proteins in Table 1, which shows that the solubilisation of WPI powder was nearly, but not totally complete. Laser light diffraction measurements on protein solutions confirmed the presence of a few insoluble aggregates in the native protein solutions with an average diameter of 30 μm, but Fig. 2 shows also that they were progressively overshadowed in the volume-weighted particle size distributions by soluble aggregates when the temperature of heat treatment was increased: beyond 70 °C, only soluble aggregates can be seen in Fig. 2, even though centrifugation shows an increase of the fraction of insoluble protein aggregates in Table 1. The average size of the soluble aggregates increased from about 200 to 600 nm with the temperature of heat treatment between 70 °C and 90 °C, and the peak narrowed at the same time, as expected. It can be pointed out that, contrary to protein denaturation, similar results had been observed by Nicorescu et al. (2009a) on protein aggregation in this range of temperature, even though protein content was lower and the technology used for thermal treatment differed.

Thirdly, DLS and SEC data on supernatants confirmed the formation of soluble protein aggregates due to heat treatment at 70 °C and above (Fig. 3). On the basis of peak area, the fraction of soluble aggregates was estimated from SEC data as in Nicorescu et al. (2008a) and is reported in Table 1: as it can be seen in Fig. 3a, the peaks moved progressively towards shorter elution times with the temperature of heat treatment, i.e. the proportion of soluble aggregates increased and reached 12–14% of the total protein content for a thermal treatment at 80 °C. As before for insoluble aggregates, this proportion varied only slightly between 80 °C and 90 °C. Complementary information from DLS curves (Fig. 3b) is that native whey proteins dimers presenting typically an average diameter of 8 nm (Mourouzidis-Mourouzis & Karabelas, 2006) could be clearly identified only for native protein solutions: their peak is progressively overshadowed by soluble aggregates

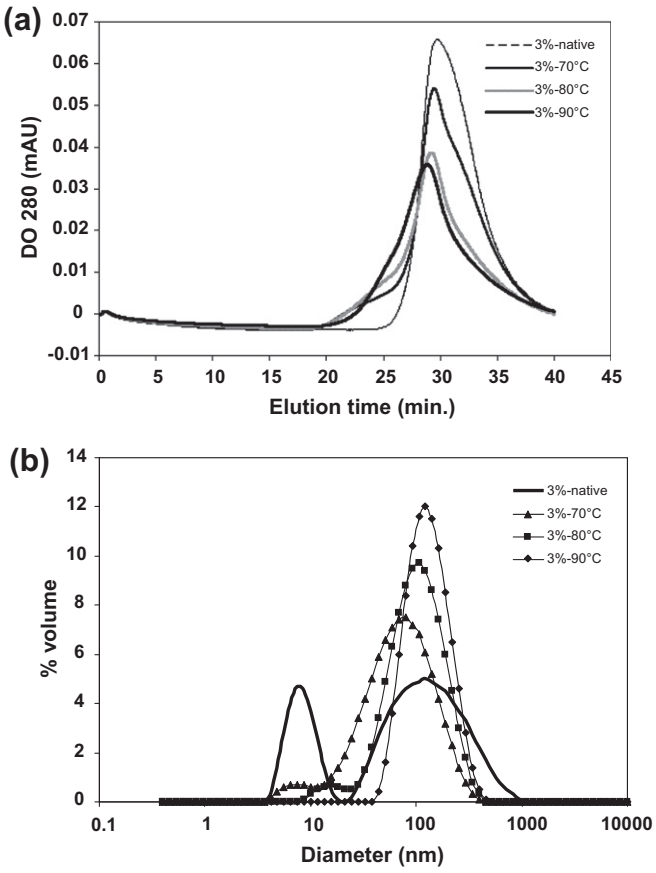

Fig. 3. Analysis of protein aggregation in supernatants from native and heat-treated WPI solutions: (a) SEC data; (b) DLS data.

formed by heat treatment and vanishes at 80 °C in Fig. 3b. DLS curves give also access to an estimation of the hydrodynamic diameter of soluble protein aggregates (reported in Table 1). This increased with heat treatment, while the width of the peak decreased, in qualitative agreement with Fig. 2. However, average diameters differed between Figs. 2 and 3b, DLS providing always the lowest values. A simple explanation is that laser light diffraction truncates the size distribution below 50 nm, which leads to an overestimation of the average size, whereas centrifugation before DLS measurements truncates the size distribution above 500 nm, which leads on the opposite to an underestimation. Again, these trends were similar to those observed by Nicorescu et al. (2008a), despite the differences between the conditions applied.

Finally, surface tension curves vs. time (data not shown) confirmed that native proteins always presented a lower surface tension than the heat-treated samples, in agreement with previous works (Nicorescu et al., 2008a, Nicorescu et al., 2009a), which confirms that the affinity of protein aggregates towards air interfaces is weaker. This behaviour is illustrated in Table 1 by σ values measured after 3 h and has always been attributed to the slower diffusion-controlled adsorption of protein aggregates coupled to their higher difficulty to undergo conformational changes at air/water interfaces (see, e.g. Davis & Foegeding, 2004; Miller et al., 1998).

As a conclusion, dynamic heat treatment promotes simultaneously the denaturation and the aggregation of whey proteins. For the degree of denaturation, this work starts from native proteins up to nearly complete denaturation at 80 °C or above. For aggregation, both the fractions of soluble and insoluble aggregates increase with the temperature of thermal treatment, but both tend to a plateau value between 80 °C and 90 °C. Conversely, surface

tension rises sharply when heat treatment is applied, but does not differ significantly when temperature is increased from 70 °C to 90 °C. As aggregate size increases at the same time, this explains why the effect of heat treatment on protein properties is quite complex and why contradictory results can be found in the literature. Now, the objective is to analyse and better understand the evolution of the performance of continuous food aeration on the basis of these results.

3.2. Analysis of continuous aeration

As a preliminary result, the viscosity of the xanthan/protein mixture was shown to be similar for all the recipes, regardless of the heat treatment applied to proteins. Indeed, viscosity was governed by the presence of 0.35% w/v xanthan, while the influence of protein aggregation and denaturation was insignificant on viscosity.

3.2.1. Overrun

For the conditions used in this work, overrun was independent of the heat treatment applied; consequently, "blow-by" characterised by a slug flow regime in the outlet stream appeared only as a function of the operating conditions of aeration. Table 2 summarises typical results obtained for native proteins that illustrate general trends. At atmospheric pressure, when residence time τ was equal to 120 s, overrun reached always 200%, which corresponded to a complete incorporation of the gas phase, whatever the rotation speed between 400 and 1600 rpm and heat treatment. First, a reduction of residence time at constant G/L ratio required higher rotation speed to achieve $\Phi = 200\%$. If one considers that the mechanical energy required for dispersing the gas phase is intrinsically linked to the recipe and to the geometry of the mixing head, lower τ values enforce higher power and therefore higher N values, which agrees with observations. Then, for $P = 2$ bars, blow-by was always observed for $\tau = 120$ s, except for $N = 1600$ rpm; however, when τ was decreased to 40 s, 100% aeration efficiency was again achieved. Actually, pressurised conditions have three counterbalancing effects: firstly, they decrease the effective volume of the gas phase in the mixing head which should favour gas dispersion, secondly, they increase the actual residence time in the mixing head (it is about $9\tau/5$ in this work when gauge pressure is 2 bars) which can simultaneously enhance bubble breakup and favour bubble collision and recoalescence, and thirdly, the aerated structure can collapse rapidly due to gas expansion downstream to the backpressure valve. For $\tau = 120$ s, the negative effects prevail. This behaviour corresponds apparently to the continuous version of the "overwhipping" phenomenon, described in batch aeration when whipping time is too long (Jakubczyk & Niranjan, 2006; van Aken, 2001), which is mainly due to bubble recoalescence when the actual residence time is $9\tau/5$. Consequently, the positive influence of high N values at $\tau = 120$ s stems probably from the fact that bubble recoalescence is overshadowed by bubble breakup at high N values, as already observed for droplets (see, e.g. Vinckier, Moldenaers, Terracciano, & Grizzuti, 1998). For $\tau = 40$ s, *Eff* was 100%, mainly because the increase of the actual residence time due to pressurised conditions is counterbalanced by the decrease of the apparent residence time τ from 120 s to 40 s. This result is in perfect agreement with data already reported by Labbafi et al. (2005) on aerated dairy desserts: under pressure, gas dispersion in the RS unit is easier, but must be achieved at a lower apparent residence time in order to avoid overwhipping.

Finally, heat treatment seems to have no effect on these trends. The loss of foamability, often reported in the literature when protein denaturation is complete on the basis of proteins foams formed in batch kitchen mixers (see, e.g. Nicorescu et al., 2009a) or bubbling techniques (see, e.g. Nicorescu et al., 2009b) does not seem to play any role on overrun under steady state conditions with $\Phi = 200\%$ as the objective. Aeration in the RS unit appears therefore to be robust and flexible, as it can be achieved in a large range of operating conditions and it is possible to increase productivity by working under pressure at lower τ values.

Table 2
Evolution of the aeration efficiency *Eff* for native proteins as a function of operating conditions of aeration.

N (rpm)	Atmospheric pressure		$P = 2$ bars	
	$\tau = 120$ s	$\tau = 40$ s	$\tau = 120$ s	$\tau = 40$ s
400	100%	55%	BB	100%
800		100%	BB	
1200		100%	BB	
1600		100%	100%	

BB: blow-by is so high that accurate density measurements could not be carried out.

3.2.2. Microstructure analysis

Only conditions for which $\Phi = 200\%$ will be considered. Contrary to overrun, bubble size distributions after aeration depend both on aeration conditions and upstream heat treatment. The effect of aeration parameters, especially rotation speed, is however the most important, regardless of heat treatment, as can be seen from a comparison between Fig. 4a1 and Fig. 4b1. Increasing N always contribute to decrease sharply the average bubble size and to narrow the bubble size distribution. This result is in good agreement with those obtained by Indrawati et al. (2008a, 2008b). Similarly, pressurised conditions lead to a further decrease of Sauter diameter and provided more uniform size distributions (see Fig. 4b2 vs. Fig. 4a1). Conversely, increasing τ lead to larger d_{32} values and size distributions (see Fig. 4b3 vs. Fig. 4(b2)), regardless of static pressure and heat treatment. Finally, for thermal treatment, a progressive decrease of d_{32} was observed, together with a narrowing of the size distribution when temperature was increased (Fig. 4a), although this remained limited in comparison to the respective effects of N, P and τ. It should also be mentioned that no significant difference emerged between micrographs taken after 80 °C and 90 °C heat treatments, which agrees with the evolution of protein properties in Table 1.

As a conclusion, bubble size is more sensitive than overrun to aeration conditions and heat treatment. Data obtained by continuous foaming on the RS unit are in good agreement with those observed usually reported in batch whipping (see, e.g. Nicorescu et al., 2009a) for the heat treatment of proteins: this contributes to the increase of the number of bubbles in the aerated microstructure at constant overrun, leading to smaller bubble sizes and more uniform size distributions. These trends suggest that important positive changes should be observed, both on foam texture and foam stability against drainage. However, the influence of aeration conditions remains predominant on d_{32}: rotation speed is the key parameter, while pressure enables a further decrease of bubble size and an increase of productivity, as it must be accompanied by a decrease of τ.

3.2.3. Foam stability

The strong effect of aeration conditions on bubble size suggests that the stability of the aerated structure would depend mainly on aeration parameters. This is partly true, i.e. when d_{32} higher than 200 μm, e.g. due to low rotation speed, foam stability fell. When operating conditions ensured that d_{32} was lower than 200 μm, the analysis of foam collapse experiments appeared more complex. For example, Fig. 5a highlights that the strong effect of pressurised aeration on bubble size when $N = 1600$ rpm in Fig. 4 does not really prevent foam collapse, contrary to expectations. Conversely, the

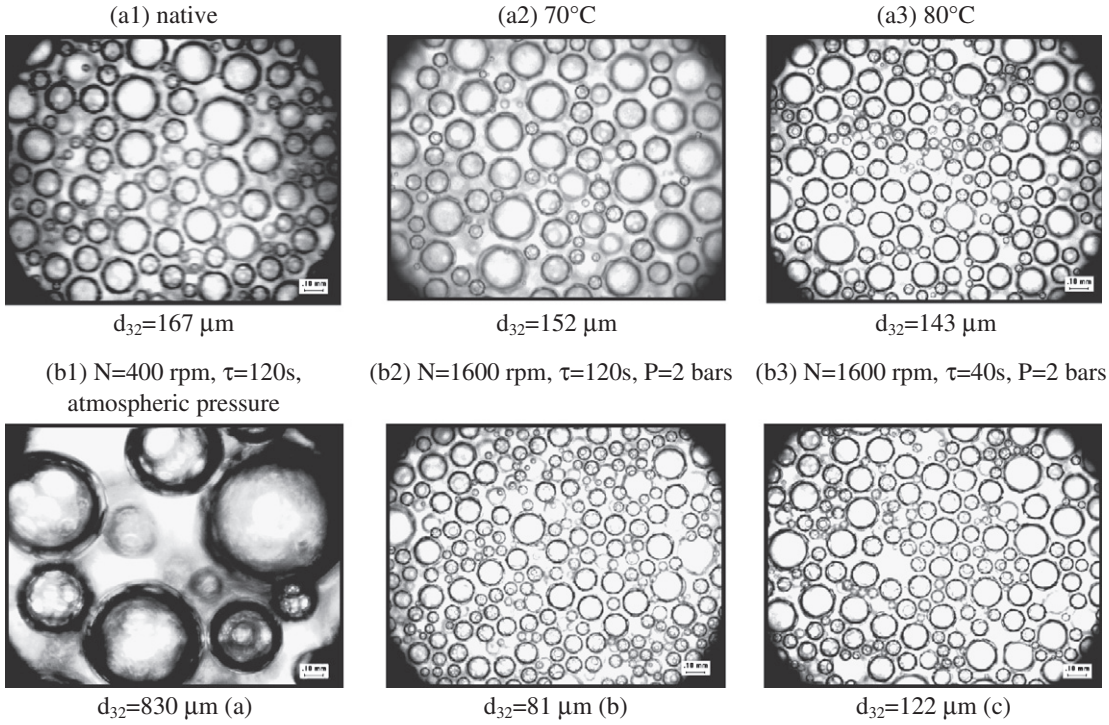

Fig. 4. Foam micrographs: (a) as a function of the heat treatment temperature (N = 1600 rpm; τ = 120 s); (b) as a function of operating conditions for native proteins.

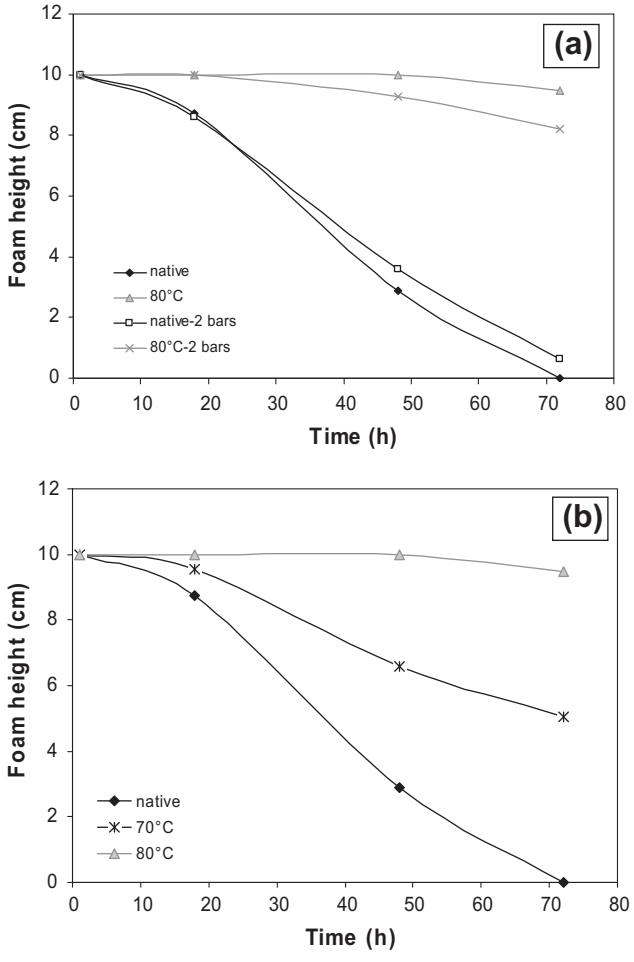

Fig. 5. Analysis of foam collapse vs. time (τ = 120 s, N = 1600 rpm).

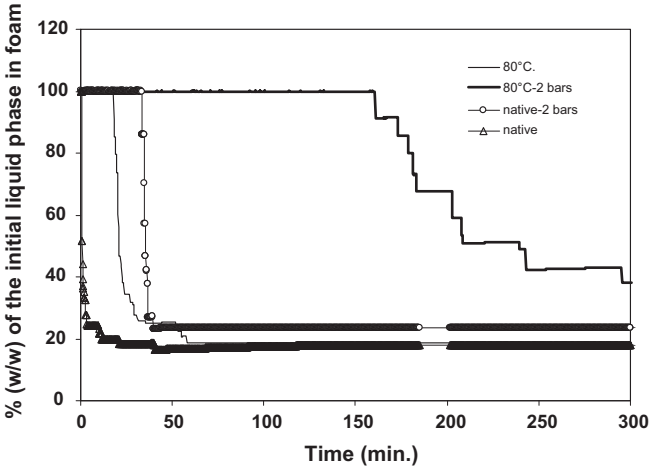

Fig. 6. Analysis of foam drainage vs. time (τ = 120 s, N = 1600 rpm).

positive impact of heat treatment on foam collapse is striking in Fig. 5, although overrun was constant and d_{32} varied only slightly in Fig. 4a. In Fig. 5b, foam stability increased progressively with treatment temperature up to 80 °C, while results at 90 °C were similar to those at 80 °C (data not shown). The data of drainage experiments exhibited the same pattern, with only a few differences. In particular, the stabilizing influence of operating pressure appeared to be more marked in Fig. 6 on the delay before which the first drop drained was detected.

Finally, all these results agree with numerous recent data that emphasise the key role of soluble protein aggregates of β-lactoglobulin and WPI produced under thermal treatment on bubble stability in foams (Davis & Foegeding, 2004; Nicorescu et al., 2008b, Nicorescu et al., 2009a; Rullier et al., 2008; Zhu & Damodaran, 1994), even though they all used batch aeration. As before, they contradict surface tension measurements that predict

a decrease of foam stability after heat treatment (Table 1). Two different possible and coexisting mechanisms have been proposed to explain these trends: (1) protein aggregates adsorb at the interface and increase the interfacial viscoelasticity, thus enhancing foam stabilization (Davis & Foegeding, 2004; Rullier et al., 2008); (2) the aggregates which do not adsorb to the interface can become confined into foam films and promote a percolation process, leading to the formation of a gel-like network which might slow down liquid drainage (Schmitt et al., 2007). Our results cannot allow a clear identification of which effect prevails. However, the high liquid content of our aerated products (33% v/v) and the strong difference between the drainage curves of foams obtained under pressurised conditions in Fig. 6 indicate that protein aggregates may act both in the continuous phase and at the interface, as d_{32} was nearly identical for both products (81 μm and 87 μm for native and 80 °C treatment, respectively). It is however clear that, as the foam becomes dryer, the influence of interfacial viscoelasticity increases and that it probably governs the effect of heat treatment on the collapse curves in Fig. 5.

As a conclusion, experimental data highlight that protein heat treatment is able to improve the stability of aerated food manufactured in a continuous process under steady state conditions, both against drainage and collapse. In particular, an amount of about 10–15% soluble aggregates (Table 1) seems to improve drastically foam stability. This confirms laboratory experiments from the literature, based classically on 600% to 1000% overrun foams. However, the impact of heat treatment cannot be predicted quantitatively from batch experiments because this remains intrinsically linked to aeration conditions, first rotation speed, and to a lesser extent operating pressure: indeed, it seems that bubble size must be lower than a critical value before the influence of heat treatment becomes effective, which depends mainly on aeration conditions.

3.2.4. Foam texture

In this work, foam texture was estimated using the viscoelastic shear storage modulus (G'), which is a bulk texture parameter of the aerated structure. G' values at 1 Hz and 0.5% strain were used for comparison purpose. Roughly, G' increased with rotation speed (Fig. 7) and decreased when residence time decreased (data not shown) for native and heat-treated proteins. This was clearly expected, as G' depends on bubble size d_{32} at constant overrun. Indeed, in dry surfactant foams, G' scales as $1/d_{32}$. Although this exact behaviour cannot be expected in complex real foods and/or when $\Phi = 200\%$, the increase of G' when d_{32} decreases remains a rule in the literature not only for protein foams (Nicorescu et al., 2008b, Nicorescu et al., 2009a), but also for complex food (e.g. an aerated white sauce in Thakur et al., 2003). The effect of operating pressure on G' is more complex, as it favours blow-by when $\tau = 120$ s, which does not allow to compare all the conditions studied at constant overrun. As a result, G' was far lower at $P = 2$ bar for foams with native proteins up to $N = 1200$ rpm, whereas G' had the same order of magnitude for both pressure conditions when $N = 1600$ rpm, which correlates to the occurrence of blow-by up to 1200 rpm in Table 1.

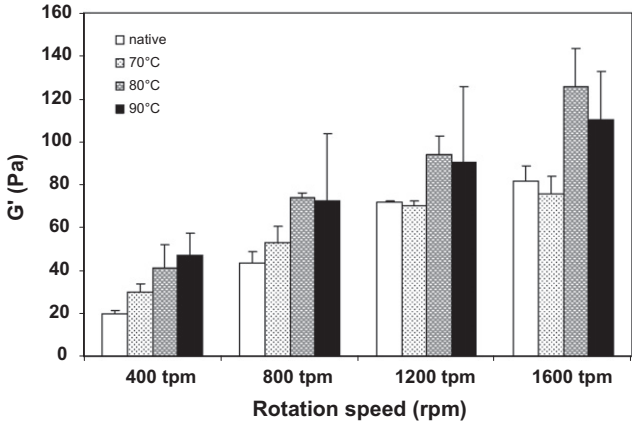

Fig. 7. Analysis of the texture of aerated food on the basis of the shear storage modulus G' at 1 Hz and 0.5% strain ($\tau = 120$ s, atmospheric pressure).

More interesting is the influence of the thermal treatment on G', plotted in Fig. 7 as a function of rotation speed. G' was significantly higher at constant rotation speed and overrun when the temperature of heat treatment was 80 °C or 90 °C for N values above 800 rpm, i.e. when d_{32} became smaller than 200 μm. This was accompanied by an increase of the uncertainty on G' values, mainly resulting from the increased difficulty for sample set-up on the rheometer plate as far as the solidity of the sample increased. This result is in good agreement with literature data on heat-treated proteins in dry WPI foams formed under batch conditions. For example, Nicorescu et al. (2009a) had shown that G' strongly increased for WPI heat-treated above 80 °C containing 10% soluble aggregates; similarly, Davis and Foegeding (2004) had reported an increase of yield stress, a rheological parameter strongly linked to G' for foams, when heat treatment was applied, but they observed also a maximum of yield stress at about 50% polymerised WPI, which has not been confirmed for G' in the literature.

However, it appears clearly that the strongly improved elasticity of protein-stabilised foams emerging from laboratory data cannot be extrapolated to continuous aeration because the increase of G' in Fig. 7 remains rather limited in comparison to that reported for dry foams. This behaviour is not surprising if one considers that the main role of protein aggregates is to enhance the interfacial viscoelasticity; this governs G' in dry foams with overrun above 1000% (Nicorescu et al., 2009a), but when overrun is only 200%, the role of proteins aggregates on bulk rheology and foam texture is necessarily weaker. This explains also why the effect of heat treatment appears only when d_{32} is lower than 200 μm, i.e. when the interfacial area is high enough so that interfacial rheology may act on bulk rheology.

As a conclusion, upstream heat treatment of protein solutions enhances the elasticity and the solidity of foams. In relation to previous works, this may be related to the proportion of soluble aggregates (Table 1). However, in continuous aeration, this behaviour depends widely on the desired overrun and on the bubble size that can be achieved, i.e. on the aeration conditions, as the influence of N is as high as that of heat treatment in Fig. 7. Indeed, contrary to batch process, overrun is fixed a priori by the G/L ratio; similarly, residence time is usually low in continuous aerators and bubble size is therefore a strong function of rotation speed and pressure. As heat-treated proteins act mainly on the air/water interface, a high interfacial area at constant Φ is therefore required, i.e. low d_{32} values, which can be obtained only by optimizing N and P in the RS unit.

3.2.5. Discussion on heat treatment

Despite the abundant literature on the thermal denaturation and aggregation of whey proteins, there is still much to understand on the influence of heat treatment on the properties of aerated foods, especially when aeration is carried out in continuous devices. Using a plate heat exchanger for thermal treatment and a rotor–stator device with the objective of 200% overrun, similarities and discrepancies have been highlighted with results obtained from laboratory experiments based on batch heaters, kitchen mixers or bubbling techniques. In summary, the trends observed in this work correspond roughly to those reported for dry foams in the literature, but they are always highly attenuated, except for stability against drainage and collapse. In practice, heat treatment seems to play a key role only when bubble size is below a critical value. This value is probably linked to interfacial area, and it should

therefore decrease as far as the desired overrun is lower. This strongly links the effect of heat treatment to the performance of the mixing head and to the aeration conditions, which also highlights the complex interplay between the process parameters of aeration and recipe variables on the properties of aerated food products.

4. Conclusions

The continuous aeration of a WPI/xanthan mixture, with WPI heat-treated dynamically using a plate heat exchanger, has been investigated using a rotor–stator unit in order to gain a better understanding of the influence of protein heat treatment on aeration performance. The interplay between the heat treatment acting on the foaming properties of the continuous phase and the process parameters of aeration has also been analysed with the objective to manufacture an aerated food that does not have the structure of a dry foam (Φ = 200%). The key role of aeration conditions on overrun, bubble size, foam stability and foam texture, was emphasised. Indeed, overrun and bubble sizes were governed by the operating conditions of aeration, which influenced also widely texture and stability. Rotation speed emerged as the key parameter, but the complex interplay between residence time and operating pressure was also highlighted. For heat treatment, the same trends as in dry foams were obtained, i.e. bubble size reduction and texture enhancement, but they were highly attenuated, except on the stability of the aerated structure. These positive effects were attributed to the presence of soluble protein aggregates. As already reported in the literature, a dynamic 80 °C–300 s heat treatment with about 10% soluble protein aggregates corresponded to the best compromise, as no improvement could be obtained by a further temperature increase. Although a percolation mechanism could not be excluded, the effect of heat treatment seemed to stem mainly from the presence of the soluble protein aggregates at the air/water interfaces. These effects were therefore enhanced by the decrease of the average bubble size at constant overrun, i.e. when the operating conditions of aeration were optimised in order to reduce d_{32}. This result highlights that the role of ingredients can be varied by acting on aeration parameters, which explains why batch experiments in a kitchen mixer are unable to predict quantitatively the effect of ingredients in continuous aeration. Finally, the complex interplay between process and recipe variables also explains partly why contradictory results can be found in the literature.

Acknowledgements

The authors gratefully acknowledge the financial and material support from *IDI Ingredients* (Arras, France).

References

Balerin, C., Aymard, P., Ducept, F., Vaslin, S., & Cuvelier, G. (2007). Effect of formulation and processing factors on the properties of liquid food foams. *Journal of Food Engineering, 78*, 802–809.

Bee, R. D., Clement, A., & Prins, A. (1987). Behaviour of an aerated food model. In E. Dickinson (Ed.), *Food emulsions and foams* (pp. 128–143). London: Royal Society of Chemistry.

Bench, J. B., Johnson, R., Hamilton, C., Gooch, J., & Wright, J. R. (2004). Adivin self-associates with boric acid gel suspensions: An affinity boron carrier that might be developed for boron neutron-capture therapy. *Journal of Colloid and Interface Science, 270*, 315–320.

Damodaran, S. (1997). Protein stabilized foams and emulsions. In S. Damodaran & A. Paraf (Eds.), *Food proteins and their applications* (pp. 77–94). New York: Marcel Dekker Inc..

Davis, J. P., & Foegeding, E. A. (2004). Foaming and interfacial properties of polymerized whey protein isolate. *Food Chemistry and Toxicology, 69*, 404–410.

Djelveh, G., & Gros, J. B. (1995). Estimation of physical properties of foamed foods using energy dissipation in scraped-surface heat exchangers. *Journal of Food Engineering, 26*, 45–56.

Foegeding, E. A., Luck, P. J., & Davis, J. P. (2006). Factors determining the physical properties of protein foams. *Food Hydrocolloids, 20*, 284–292.

Hanselmann, W., & Windhab, E. (1999). Flow characteristics and modeling of foam generation in a continuous rotor–stator mixer. *Journal of Food Engineering, 38*, 393–405.

Indrawati, L., Wang, Z., & Narsimhan, G. (2008b). Characterization of protein stabilized foam formed in a continuous shear mixing apparatus. *Journal of Food Engineering, 88*, 456–465.

Indrawati, L., Wang, Z., Narsimhan, G., & Gonzalez, J. (2008a). Effect of processing parameters on foam formation using a continuous system with a mechanical whipper. *Journal of Food Engineering, 88*, 65–74.

Jakubczyk, E., & Niranjan, K. (2006). Transient development of whipped cream properties. *Journal of Food Engineering, 77*, 79–83.

Kazmierski, M., & Correding, M. (2003). Characterization of soluble aggregates from whey protein isolate. *Food Hydrocolloids, 17*, 685–692.

Labbafi, M., Bouaouina, H., Vial, C., Djelveh, G., Picgirard, L., Casalinho, J., et al. (2005). Impact de la technologie et des conditions du foisonnement sur l'élaboration de mousses laitières de type «topping». *Science des Aliments, 25*, 381–395.

Labbafi, M., Thakur, R. K., Vial, C., & Djelveh, G. (2007). Development of an on-line optical method for assessement of the bubble size and morphology in aerated food products. *Food Chemistry, 102*, 454–465.

Marshall, R. T., Goff, H. D., & Hartel, R. W. (2003). *Ice cream* (6th ed.). New York: Kluwer Academic, Plenum Publishers.

Miller, R., Krägel, J., Wüstneck, R., Wilde, P. J., Li, J. B., Fainerman, V. B., et al. (1998). Adsorption kinetics and rheological properties of food proteins at air/water and oil/water interfaces. *Nahrung, 42*, 225–228.

Mourouzidis-Mourouzis, S. A., & Karabelas, A. J. (2006). Whey protein fouling of microfiltration ceramic membranes—Pressure effects. *Journal of Membrane Science, 282*, 124–132.

Müller-Fischer, N., & Windhab, E. J. (2005). Influence of process parameters on microstructure of food foam whipped in a rotor–stator device within a wide static pressure range. *Colloids and Surface A: Physicochemical and Engineering Aspects, 263*, 353–362.

Narchi, I., Vial, C., & Djelveh, G. (2007). Influence of bulk and interfacial properties and operating conditions on continuous foaming operation applied to model media. *Food Research International, 40*, 1069–1079.

Nicorescu, I., Loisel, C., Vial, C., Riaublanc, A., Djelveh, G., Cuvelier, G., et al. (2008a). Combined effect of dynamic heat treatment and ionic strength on the properties of whey protein foams – Part I. *Food Research International, 41*, 707–713.

Nicorescu, I., Loisel, C., Vial, C., Riaublanc, A., Djelveh, G., Cuvelier, G., et al. (2008b). Combined effect of dynamic heat treatment and ionic strength on the properties of whey protein foams – Part II. *Food Research International, 41*, 980–988.

Nicorescu, I., Loisel, C., Vial, C., Riaublanc, A., Djelveh, G., Cuvelier, G., et al. (2009a). Effect of dynamic heat treatment on the physical properties of whey protein foams. *Food Hydrocolloids, 23*, 1209–1219.

Nicorescu, I., Riaublanc, A., Loisel, C., Vial, C., Djelveh, G., Cuvelier, G., et al. (2009b). Morphology and functionality of the self-assemblages induced by dynamic heat-treatment. Impact on the physical properties of whey protein foams. *Food Research International, 42*, 1434–1445.

Rullier, B., Novales, B., & Axelos, M. (2008). Effect of protein aggregates on foaming properties of β-Lactoglobulin. *Colloids and Surfaces A: Physicochemical and Engineering Aspects, 330*, 96–102.

Saint-Jalmes, A., Peugeot, M. L., Ferraz, H., & Langevin, D. (2005). Differences between protein and surfactant foams: Microscopic properties, stability and coarsening. *Colloids and Surfaces A: Physicochemical and Engineering Aspects, 263*, 219–225.

Schmitt, C., Bovay, C., Rouvet, M., Shojaei-Rami, S., & Kolodziejczyk, E. (2007). Whey protein soluble aggregates from heating with NaCl: Physicochemical, interfacial, and foaming properties. *Langmuir, 23*, 4155–4166.

Thakur, R. K., Vial, C., & Djelveh, G. (2003). Influence of operating conditions and impeller design on the continuous manufacturing of food foams. *Journal of Food Engineering, 60*, 9–20.

Thakur, R. K., Vial, C., & Djelveh, G. (2005). Combined effects of process parameters and composition on foaming of dairy emulsions at low temperature in an agitated column. *Journal of Food Engineering, 68*, 335–347.

Unterhaslberger, G., Schmitt, C., Shojaei-Rami, S., & Sanchez, C. (2007). β-lactoglobulin aggregates from heating with charged cosolutes: Formation, characterization and foaming. In E. Dickinson & M. E. Leser (Eds.), *Food colloids: Self-assembly and material science* (pp. 175–191). Cambridge: Royal Society of Chemistry.

Van Aken, G. A. (2001). Aeration of emulsions by whipping. *Colloids and Surfaces A: Physicochemical and Engineering Aspects, 190*, 333–354.

Vinckier, I., Moldenaers, P., Terracciano, A. M., & Grizzuti, N. (1998). Droplet size evolution during coalescence in semiconcentrated model blends. *AIChE Journal, 44*, 951–958.

Walstra, P. (2003). *Physical chemistry of foods*. New York: Marcel Dekker.

Zhu, H., & Damodaran, S. (1994). Heat-induced conformational changes in whey protein isolate and its relation to foaming properties. *Journal of Agricultural and Food Chemistry, 42*, 846–855.